Trabajo de Fin de Grado

Bose-Einstein Condensates of Dilute Alkali Gases

Andrea Perdomo García
Director: Vicente Delgado Borges
Universidad de La Laguna

San Cristóbal de La Laguna, 4 de julio de 2017

Contents

Resumen

Los condensados de Bose-Einstein han sido uno de los sistemas más estudiados en los últimos años, desde que en 1995, se logró por primera vez un experimento en el que se generaran con éxito condensados prácticamente puros. No es de extrañar el interés que hay sobre este estado de la materia, pues se encuentra en multitud de sistemas en la naturaleza y tiene importantes aplicaciones en interferometría atómica y computación cuántica, además de ser la base del desarrollo del láser de átomos. En este trabajo desarrollamos el marco teórico usual para trabajar con condensados a temperaturas cercanas al cero absoluto, para luego, abordar el formalismo adecuado para el tratamiento de condensados alargados.

A continuación, aplicamos las ecuaciones obtenidas a una serie de condensados alargados utilizando técnicas computacionales, comparando los resultados numéricos con expresiones analíticas aplicadas al mismo problema.

1 Introduction: Objectives and Methodology

Este trabajo está dividido en dos partes principales: Un teórica formada por las Secciones 2, 3 y 4; y otra práctica, que corresponde a las Secciones 5, 6 y 7.
En la primera parte, el objetivo es introducir aspectos generales de la condensación de Bose-Einstein, tales como el concepto de condensado, las técnicas utilizadas para obtenerlos y el interés de estos sistemas. Para completar esta descripción, se deduce la ecuación de Gross Pitaevskii, que gobierna la dinámica de cualquier condensado a temperatura cero. Además, se estudia el caso de interés de los condensados alargados, desarrollando una ecuación que los describe a partir de la ecuación de Gross-Pitaevskii.
En base a las ecuaciones obtenidas, se da paso a la segunda parte del trabajo, donde se desarrolla un programa de ordenador que permita el estudio de condensados quasi-unidimensionales. Para ello, se utilizan técnicas numéricas como el método de Crank-Nicolson a la hora de escribir el código, comparando los resultados obtenidos con expresiones analíticas.

This work is divided in two main parts: Sections 2, 3 and 4, which correspond to the theoretical part; and Sections 5, 6 and 7, which correspond to the practical part. In the first part, the objective is to make an introduction about general aspects of Bose-Einstein condensation. In order to achieve this goal, some notions about this topic are expounded, such as the concept of Bose-Eintein Condensate (BEC), the ways to obtain them and the interest of these systems. Following this idea, the Gross-Pitaevskii equation (GPE), which describes a general condensate near the absolute zero, is obtained. A specific formalism is shown in order to study the interesting case of elongated condensates, whose equation is obtained.
The aim of the second part is to develop a computer program that permits the study of the dynamics of a quasi-onedimensional BEC. Numerical techniques such as the Crank-Nicolson method are used in order to write the program, which is tested by comparing the results with analytical expressions.

2 Bose-Einstein Condensation of Dilute Alkali Gases

Primero, se introduce en este apartado el concepto de condensado de Bose-Einstein, especificando las condiciones necesarias para su creación, así como sus características más importantes. Luego, se indaga con mayor profundidad en los mecanismos involucrados en la obtención de estos sistemas, explicando el proceso de enfriamiento y el papel de las trampas magneto-ópticas (dando algunos ejemplos de estas). Para acabar esta introducción, se especifican algunos campos de estudio donde los condensados tienen un papel importante y se especifican sistemas en los que se encuentran.

A Bose-Einstein condensate is a system of bosons which occupy the same single-particle state and show quantum coherence on a macroscopic scale. The achievement of such a coherent state requires specific density and temperature conditions. BECs can be understood as another state of matter.
In this work, we are interested in dilute alkali gases. These systems are particularly suitable for being cooled using laser techniques and magnetic traps, which are the best cooling techniques known nowadays. In addition, alkali atoms interact mainly via two-body elastic interactions, which allows the system remain in its gaseous state till the condensation is achieved.
In alkali gases, temperatures near absolute zero are needed to assure the system is cold enough (fractions of microkelvins or less) that all the particles are in the same single-particle state, the one of minimum energy possible before the gas solidifies. At such low temperatures, the kinetic energy of the bosons is so small that their de Broglie wavelength becomes of the order of the interparticle distance. Under these circumstances, single-particle wave functions overlap giving rise to a macroscopic condensate wave function.
Density has an important role in the experimental realization of Bose-Einstein condensation: It should be high enough to get the atomic wave functions overlap and, however, low enough to avoid the atoms to form molecules. Since BECs are metastable states of matter (with life-times typically of the order of seconds or minutes), if their atoms form molecules the gas solidifies rapidly and the life-time of the condensate is reduced.
One important characteristic that defines a BEC is that a peak in a near-zero value appears in the momentum representation as a consequence of all the particles being in their lowest energy state. Since the magnetic traps we are interested in are harmonic ones, another peak appears in the coordinate representation. For BECs trapped in uniform potentials, only the peak in the momentum representation exists.

It is not a trivial issue to obtain a BEC. Not only is important the identification of systems that are suitable for staying gaseous all the way to the BEC transition, but development of cooling and trapping techniques is also needed to reach the particular temperatures and densities required for the condensation.
The cooling method consists of two parts: Laser cooling and evaporative cooling. Laser cooling is used to pre-cool the gas. The incident photons of the laser interchange momentum with the particles of the gas in such a way that, after the scattering process, the photons have increased their momentum, decreasing the kinetic energy of the particles and cooling the gas.
After the pre-cooling, we need our gas to be trapped in a magnetic or laser field (magneto-optical trapping, MOT). This kind of trapping is used instead of a box for example, because in this latter case the gas interacts with the walls of the container, facilitating the creation of molecules, which brings the system to a solid phase. The first stage of this trapping consists in applying a weak magnetic field with laser fields. The second, consists in the use of a stronger inhomogeneous magnetic field, achieving an appropriate density which assures enough elastic collisions among the atoms.
When this density is reached, it is time to apply evaporative cooling. It consists in reducing the trap depth, allowing the most energetic atoms to scape, thus decreasing the temperature of the remainder system.
The Ioffe-Pritchard trap is an example of magnetic trap usually found in Bose-Einstein condensation. The form of the magnetic field applied in this trap is:

$$\vec{B} = B_0 \mathbb{1}_z + B' \left(\mathbb{1}_x - \mathbb{1}_y \right) + \frac{B''}{2} \left[\left(z^2 - \frac{1}{2} \left(x^2 + y^2 \right) \right) \mathbb{1}_z - xz \mathbb{1}_x - yz \mathbb{1}_y \right], \qquad (1)$$

where B_0 is the minimum of the axial magnetic field, $B' = \frac{\partial B_x}{\partial x} = -\frac{\partial B_y}{\partial y}$ and $B'' = \frac{\partial^2 B_z}{\partial z^2}$. The potential associated with a magnetic field $\vec{B}$ is $V = -\vec{\mu}\vec{B}$, where $\mu = g_F \mu_B m_F$ is the magnetic momentum induced in an atom of the condensate in the hyperfine state $|F, m_F\rangle$. This potential, can be approximated with high accuracy by the following potential:

$$V(\vec{r}) = g_F \mu_B m_F |\vec{B}| \simeq \frac{g_F \mu_B m_F}{2} \left[\left(\frac{B'^2}{B_0} - \frac{B''}{2} \right) \left(x^2 + y^2 \right) + B'' z^2 \right], \qquad (2)$$

where g_F is the Landé g-factor and μ_B is the Bohr magneton.
In general, any typical potential associated with a trap used in condensation can be approximated using a harmonic potential. In particular, as occurs in the case of the

Ioffe-Pritchard trap, it is common to work with axisymmetric potentials:

$$V(\vec{r}) = V_\perp(r_\perp) + V_z(z) = \frac{1}{2}m\left(\omega_\perp^2 r_\perp^2 + \omega_z^2 z^2\right), \tag{3}$$

where $\vec{r}_\perp = \sqrt{x^2+y^2}$ is the transversal coordinate and z is the axial coordinate. This potential is characterized by the oscillator lengths $a_\perp = \sqrt{\hbar/m\omega_\perp}$ and $a_z = \sqrt{\hbar/m\omega_z}$.
Periodic grids created using stationary lasers are the usual device in the case of optical traps, being common to find the one formed by two identical lasers beams propagating in opposite directions. In this case, the oscillating electric field is

$$\mathscr{E} = \mathscr{E}_0\left[cos\left(\omega t - kz\right) + cos\left(\omega t + kz\right)\right]\mathbb{1}_x, \tag{4}$$

where the spatial step in the grid is defined as $d = \frac{\pi}{k}$. The dipolar electric momentum induced in the atoms, generates the following effective potential:

$$V(z) = -\frac{1}{2}\mathfrak{a}(\omega)\left\langle\left|\mathscr{E}(z,t)\right|^2\right\rangle_t = V_0 cos^2(kz), \tag{5}$$

where $\mathfrak{a}(\omega)$ is the dynamical polarizability of the atoms, $\langle|\mathscr{E}(z,t)|^2\rangle_t$ is the intensity of the radiation and $V_0 = s\frac{(\hbar k)^2}{2m}$ where typically $0 < s \leqslant 20$.
Many other traps have been created, for examples the Dark Spot trap or the TOP trap, but those considered above (specially the Ioffe-Pritchard trap) are simpler and more convenient.
By changing the form of the potentials, one can generate spherical, disk-shaped or cigar-shaped condensates. In this work, we are going to study the general case of a condensate in an arbitrary potential (at $T = 0K$) and the case of the cigar-shaped potential (which will bring us to the quasi-onedimensional case).

We can find BECs everywhere in nature. Some examples are the alkali gaseous systems near the absolute zero; at higher temperatures (and densities), they can be found in neutron stars and white dwarf stars; they also appear in some cosmology theories, where we find them related to dark energy and mass; in superfluidity; and also in superconductivity, where the concept of condensation can be applied because the electrons form Cooper pairs.
Research on gaseous BECs can be divided in two main areas: The study of the atomic condensate as a coherent gas, for which it is needed as little interactions as possible (low densities) and the condensate as a many body system, for which the study of the interaction of the atoms is the goal (high densities).

In the first case, the experiments are focused on atom optics (coherent amplification of atoms or atom lasers, interference phenomena, diffraction, ...), precision studies, solitons (which are related to nonlinear phenomena in dissipative environments) and exploration of basic aspects of quantum mechanics. In the second, we find the study of vortices, which characterize the superfluid and superconducting properties of the gases. In soliton and vortex studies, it is usual to turn off the trap confining the BEC, and leave the system evolve freely for a few seconds (ballistic expansion).
Interference of atoms is analogous to the interference of light (actually, matter waves are similar to light waves), and had been studied almost since the first realization of Bose-Einstein condensation. In fact, this kind of experiments were developed in order to study the coherence of the BECs. The first experiment consisted in two condensates, created using a tool to split a condensate into two halves. The two BECs were separated and overlapped in ballistic expansion. In order to assure that the results were matter wave interference patterns, and not some kind of self-diffraction due to the sharp edge in the confinement, one of the condensates was eliminated by focusing resonant yellow light on it. In that moment, the fringes vanished, confirming that the result was indeed true interference. That was an important and remarkable outcome, since the destructive interference, in some way, means that atoms plus atoms add up to vacuum.
Amplification of atoms is called atom laser too due to its similarities with the light laser. A number of atoms pass through a BEC, which is acting as an active medium and is being illuminated by a laser light, provoking their "amplification", which is slightly different from light laser. While in light lasers we generate photons using atomic transitions, in atom amplifiers we transform the quantum state of the atoms from the active medium into the state of the input atoms. It is possible to use this device in order to amplify light, as in a light laser. Besides, this atom lasers can be used to improve the performance of atom interferometers, which are used as precise gravity and rotation sensors.

3 Gross-Pitaevskii Equation

En esta Sección se aborda la deducción de la ecuación de Gross-Pitaevskii, en base a un principio variacional. Primero, utilizando un anzat de Hartree-Fock, se obtiene el funcional de la energía, a partir del cual se deduce la ecuación para estados estacionaros. Luego se generaliza esta para estados dependientes del tiempo. Además, se interpreta la aparición del término no lineal en la ecuación estacionaria (que se identifica con el potencial químico).

3.1 The Energy Functional

As is well known, the problem of a system with more than two particles has not analytical solutions. Since for BECs the typical number of particles is over one hundred, it is necessary to simplify the Hamiltonian governing the condensate. One can approximate the interparticle interaction contribution to achieve this goal.
We are working at $T = 0K$, the energy is minimum, so one can consider that the scattering of two particles[1] corresponds to an s-wave scattering process. In these circumstances, the scattering is fully characterized by a single parameter: the scattering length a_S, which is positive in the cases we are interested in (repulsive interparticle interaction). Thus, we can choose any interaction potential provided that it leads to the same s-wave scattering length that can be measured experimentally, in particular, we take one of the form $V(\vec{r}_i - \vec{r}_j) = U_0\delta(\vec{r}_i - \vec{r}_j)$. We know from scattering theory [1] that, in the Born approximation (which, for low energies, is valid for short range potentials) the s-wave scattering length is

$$a_S = \frac{\tilde{\mu}}{2\pi\hbar^2}\int d\vec{r}_{ij}V(\vec{r}_{ij}), \tag{6}$$

where $\tilde{\mu}$ is the reduced mass of the two particles in the scattering and $\vec{r}_{ij} = \vec{r}_i - \vec{r}_j$. Substituting the reduced mass of two bosons $\tilde{\mu} = m/2$ and the chosen expression for the potential $V(\vec{r}_i - \vec{r}_j)$, we find

$$U_0 = \frac{4\pi\hbar^2 a_s}{m} \tag{7}$$

[1]The two body interaction dominates over the other ones for dilute gases [2].

Taking this into account, the Hamiltonian of the system is the following:

$$H = \sum_{i=1}^{N} \left(-\frac{\hbar^2}{2m}\Delta_i + V(\vec{r}_i) \right) + U_0 \sum_{i<j} \delta(\vec{r}_i - \vec{r}_j), \tag{8}$$

where N is the total number of particles in the condensate, $\Delta_i = \vec{\nabla}_i^2$ is the Laplace operator, and $V(\vec{r}_i)$ is the time independent external potential that confines the BEC.
Since the particles are bosons all in the same single-particle state, we can approximate the total wave function as the symmetrized product of the identical single-particle wave functions, which leads us to a Hartree-Fock anzat:

$$\psi(\vec{r}_1, ..., \vec{r}_N) = \prod_{i=1}^{N} \phi(\vec{r}_i) \tag{9}$$

Thus, the energy functional of the system is

$$E_N = \int d\vec{r}_1 ... d\vec{r}_N \left(\sum_{i=1}^{N} (-\frac{\hbar^2}{2m}\psi^*(\vec{r}_1, ..., \vec{r}_N)\Delta_i \psi(\vec{r}_1, ..., \vec{r}_N) + \right.$$

$$\left. + \psi^*(\vec{r}_1, ..., \vec{r}_N) V(\vec{r}_i) \psi(\vec{r}_1, ..., \vec{r}_N) \right) + \int d\vec{r}_1 ... d\vec{r}_N U_0 \sum_{i<j} \psi^*(\vec{r}_1, ..., \vec{r}_N)\delta(\vec{r}_i - \vec{r}_j)\psi(\vec{r}_1, ..., \vec{r}_N) \tag{10}$$

To calculate this functional, we can divide it in two contributions, one which corresponds to the sum of the single-particle energies of all the particles and the other which corresponds to the interparticle interaction.
The first contribution is given by

$$E_1 = \int d\vec{r}_1 ... d\vec{r}_N \Big(\psi^*(\vec{r}_1, ..., \vec{r}_N) h_1 \psi(\vec{r}_1, ..., \vec{r}_N) + ... + \psi^*(\vec{r}_1, ..., \vec{r}_N) h_N \psi(\vec{r}_1, ..., \vec{r}_N) \Big) =$$

$$= \int d\vec{r}_1 ... d\vec{r}_N \Big(\left|\phi(\vec{r}_2)\right|^2 ... \left|\phi(\vec{r}_N)\right|^2 \phi^*(\vec{r}_1) h_1 \phi(\vec{r}_1) + ... + \left|\phi(\vec{r}_1)\right|^2 ...$$

$$... \left|\phi(\vec{r}_{N-1})\right|^2 \phi^*(\vec{r}_N) h_N \phi(\vec{r}_N) \Big) = N \int d\vec{r} \Big(-\frac{\hbar^2}{2m}\phi^*(\vec{r})\Delta\phi(\vec{r}) + \phi^*(\vec{r}) V(\vec{r}) \phi(\vec{r}) \Big), \tag{11}$$

where we have used $h_i = -\frac{\hbar^2}{2m}\Delta_i + V(\vec{r}_i)$ and $\int d\vec{r}_i \left|\phi(\vec{r}_i)\right|^2 = 1$. This result agrees with the energy of a system of non-interacting bosons all in the same state, which is

just the number of particles times the energy of one of those bosons.
The second contribution is

$$E_2 = U_0 \int d\vec{r}_1 ... d\vec{r}_N \sum_{i<j} \psi^*(\vec{r}_1, ..., \vec{r}_N)\delta(\vec{r}_i - \vec{r}_j)\psi(\vec{r}_1, ..., \vec{r}_N) =$$

$$= U_0 \left[\iint d\vec{r}_1 d\vec{r}_2 \left|\phi(\vec{r}_1)\right|^2 \left|\phi(\vec{r}_2)\right|^2 \delta(\vec{r}_1 - \vec{r}_2) \int d\vec{r}_3 \left|\phi(\vec{r}_3)\right|^2 ... \int d\vec{r}_N \left|\phi(\vec{r}_N)\right|^2 + ... \right.$$

$$... + \int d\vec{r}_1 \left|\phi(\vec{r}_1)\right|^2 ... \int d\vec{r}_{i-1} \left|\phi(\vec{r}_{i-1})\right|^2 \iint d\vec{r}_i d\vec{r}_j \left|\phi(\vec{r}_i)\right|^2 \left|\phi(\vec{r}_j)\right|^2 \delta(\vec{r}_i - \vec{r}_j) ...$$

$$\left. ... \int d\vec{r}_N \left|\phi(\vec{r}_N)\right|^2 + ... \right] = U_0 \left[\iint d\vec{r}_1 d\vec{r}_2 \left|\phi(\vec{r}_1)\right|^2 \left|\phi(\vec{r}_2)\right|^2 \delta(\vec{r}_1 - \vec{r}_2) + \right.$$

$$+ \iint d\vec{r}_1 d\vec{r}_3 \left|\phi(\vec{r}_1)\right|^2 \left|\phi(\vec{r}_3)\right|^2 \delta(\vec{r}_1 - \vec{r}_3) + ... + \iint d\vec{r}_1 d\vec{r}_N \left|\phi(\vec{r}_1)\right|^2 \left|\phi(\vec{r}_N)\right|^2 \delta(\vec{r}_1 - \vec{r}_N) + ...$$

$$\left. ... + \iint d\vec{r}_2 d\vec{r}_3 \left|\phi(\vec{r}_2)\right|^2 \left|\phi(\vec{r}_3)\right|^2 \delta(\vec{r}_2 - \vec{r}_3) + ... \right] = U_0 \left[\int d\vec{r}_1 \left|\phi(\vec{r}_1)\right|^4 + ... \right] =$$

$$= \frac{U_0 N(N-1)}{2} \int d\vec{r} \left|\phi(\vec{r})\right|^4 \simeq \frac{U_0 N^2}{2} \int d\vec{r} \left|\phi(\vec{r})\right|^4 , \tag{12}$$

where we have used again the normalization condition $\int d\vec{r}_i \left|\phi(\vec{r}_i)\right|^2 = 1$. Since $N \gg 1$, we have approximated $N(N-1) \simeq N^2$.The number of terms of the sum corresponds to the result of combinations in pairs without repetition of indistinguishable elements, which is the combinatorial number

$$\binom{N}{2} = \frac{N!}{2!(N-2)!} = \frac{N(N-1)(N-2)!}{2(N-2)!} = \frac{N(N-1)}{2} \tag{13}$$

Finally, the energy functional is

$$E_N[\phi^*, \phi] = N \int d\vec{r} \left[-\frac{\hbar^2}{2m} \phi^*(\vec{r}) \Delta \phi(\vec{r}) + \phi^*(\vec{r}) V(\vec{r}) \phi(\vec{r}) + \frac{U_0 N}{2} \left|\phi(\vec{r})\right|^4 \right] \tag{14}$$

And the energy functional per particle reads

$$E[\phi^*, \phi] = \frac{E_N[\phi^*, \phi]}{N} \equiv \int \mathcal{E}\left(\phi^*, \phi\right) d\vec{r} \tag{15}$$

3.2 Stationary Gross-Pitaevskii Equation

We will use a variational principle based on the energy functional (15) to find the wave function that minimizes the energy. Because the wave functions are normalized, we introduce, using a Lagrange multiplier, the constrain $\int d\vec{r}\,|\phi(\vec{r}_i)|^2 = 1$ into the energy functional. The result is

$$E'[\phi^*,\phi] = \int d\vec{r}\left[\mathcal{E}(\phi^*(\vec{r}),\phi(\vec{r})) - \eta\,|\phi(\vec{r})|^2\right] \equiv \int \mathcal{E}'(\phi^*(\vec{r}),\phi(\vec{r}))d\vec{r} \tag{16}$$

We can take either $\phi^*(\vec{r})$ or $\phi(\vec{r})$ as the "trajectory variable" in phase space [3], so we use $\phi^*(\vec{r})$ for simplicity, because the functional does not depend on $\vec{\nabla}\phi^*(\vec{r})$, which means that the Euler-Lagrange equations $\vec{\nabla}\frac{\partial\mathcal{E}'}{\partial\left(\vec{\nabla}\phi^*\right)} - \frac{\partial\mathcal{E}'}{\partial\phi^*} = 0$ reduce to

$$\frac{\partial\mathcal{E}'}{\partial\phi^*} = 0 \rightarrow \frac{\partial}{\partial\phi^*}\left[(-\frac{\hbar^2}{2m}\phi^*(\vec{r})\Delta\phi(\vec{r}) + \phi^*(\vec{r})V(\vec{r})\phi(\vec{r})) + \right.$$

$$\left. + \frac{NU_0}{2}\,|\phi(\vec{r})|^4 - \eta\,|\phi(\vec{r})|^2\right] = 0 \tag{17}$$

Thus, after performing the partial derivative, one finally obtains

$$\left[-\frac{\hbar^2}{2m}\Delta + V(\vec{r}) + U_0N\,|\phi(\vec{r})|^2 - \eta\right]\phi(\vec{r}) = 0 \tag{18}$$

The chemical potential μ satisfies the relation $\frac{\partial E_N}{\partial N} = \mu$. From Eq. (18), we have

$$\eta = \langle\phi|\,H\,|\phi\rangle = \int d\vec{r}\phi^*\left(-\frac{\hbar^2}{2m}\Delta + V + U_0N\,|\phi|^2\right)\phi \tag{19}$$

Performing the derivative $\frac{\partial E_N}{\partial N}$ with E_N given by Eq. (14), one obtains

$$\frac{\partial E_N}{\partial N} = \int d\vec{r}\phi^*\left(-\frac{\hbar^2}{2m}\Delta + V + U_0N\,|\phi|^2\right)\phi, \tag{20}$$

which is just the expression for η found above, so it follows that $\frac{\partial E_N}{\partial N} = \eta$. This allows us to identify the Lagrange multiplier η as the chemical potential μ of the condensate. This chemical potential is the amount of energy needed to remove or add one particle to the condensate. With this, we find

$$\left(-\frac{\hbar^2}{2m}\Delta + V(\vec{r}) + U_0N\,|\phi(\vec{r})|^2\right)\phi(\vec{r}) = \mu\phi(\vec{r}), \tag{21}$$

where we can see that because of the nonlinearity of the Gross-Pitaevskii Hamiltonian, its stationary states correspond to well defined values of the chemical potential (instead of the energy, as occurs in linear systems).

3.3 Time Dependent Gross-Pitaevskii Equation

Now that we have obtained the GPE for stationary states, we may look for the corresponding time dependent equation. Such equation can be deduced analogously to the stationary one, by starting from the energy per particle functional $E[\Psi^*, \Psi]$ for time dependent states $\Psi(\vec{r}, t)$ normalized to unity, and using the variational principle [2, 4]

$$i\hbar\frac{\partial}{\partial t}\Psi = \frac{\delta E}{\delta \Psi^*} \tag{22}$$

The derivative of a functional of the form $E[\Psi^*] = \int d\vec{r}\mathcal{E}(\Psi^*, \vec{\bigtriangledown}\Psi^*)$ is defined as

$$\frac{\delta E[\Psi^*]}{\delta \Psi^*} := \frac{\partial \mathcal{E}}{\partial \Psi^*} - \vec{\bigtriangledown}\frac{\partial \mathcal{E}}{\partial(\vec{\bigtriangledown}\Psi^*)} \tag{23}$$

Since $\mathcal{E}$ does not depend on $\vec{\bigtriangledown}\Psi^*$, we finally get

$$\frac{\delta E}{\delta \Psi^*} = \frac{\partial \mathcal{E}}{\partial \Psi^*} \rightarrow i\hbar\frac{\partial}{\partial t}\Psi = \frac{\partial \mathcal{E}}{\partial \Psi^*} \tag{24}$$

Using Eq. (24) and the energy functional (15), one obtains

$$\left(-\frac{\hbar^2}{2m}\Delta + V(\vec{r}) + U_0 N\left|\Psi(\vec{r}, t)\right|^2\right)\Psi(\vec{r}, t) = i\hbar\frac{\partial}{\partial t}\Psi(\vec{r}, t), \tag{25}$$

which is the time-dependent Gross-Pitaevskii equation governing the dynamics of dilute BECs at temperatures near absolute zero. It is easy to see that for stationary states $\Psi(\vec{r}, t) = \phi(\vec{r})e^{-i\mu t/\hbar}$, Eq. (25) reduces to Eq. (21).

4 Highly Elongated Condensates

En este apartado, a partir de la ecuación de Gross-Pitaevskii se obtiene la ecuación que gobierna la dinámica de condensados muy alargados (caso quasi-unidimensional), utilizando la aproximación adiabática. Para determinar la forma completa de la ecuación, se identifica en ella el término de potencial químico local $\mu_\perp$ y se obtiene una expresión para este, a partir de cálculo variacional. Los resultados obtenidos serán utilizados para la parte práctica del trabajo.

4.1 Quasi-1D Equation of Motion

In this Section, we consider a BEC in a highly elongated trap. In these traps, the transverse motion is much faster than the axial one ($\omega_\perp \gg \omega_z$), so we can use an adiabatic approximation. In this regard, we consider that the transverse motion adjusts instantaneously to the axial configuration. Thus, we can factorize the condensate wave function as the product of an axial wave function and a transverse wave function.
Taking these considerations into account, the wave function describing the quasi-onedimensional condensate can be written as

$$\Psi(\vec{r},t) = \varphi(\vec{r}_\perp; z, t)\Phi(z,t) \equiv \varphi(\vec{r}_\perp; n_1(z,t))\Phi(z,t), \tag{26}$$

where we have specified that the dependence of φ on the parameters z and t is only through $n_1(z,t)$, advancing later results. The parameter $n_1(z,t)$ is the local condensate density per unit length characterizing the axial configuration, which is defined as

$$n_1(z,t) = N \int d\vec{r}_\perp \left|\Psi(\vec{r})\right|^2 \tag{27}$$

Since we normalize the transverse wave function as $\int d\vec{r}_\perp \left|\varphi(\vec{r}_\perp; n_1)\right|^2 = 1$, we find for $n_1(z,t)$

$$n_1(z,t) = N\left|\Phi(z,t)\right|^2 \tag{28}$$

We are interested in cases where the relation $\mu \gtrsim \hbar\omega_\perp \gg \hbar\omega_z$ is fulfilled too. In situations where $\mu \gg \hbar\omega_\perp \gg \hbar\omega_z$, the Thomas-Fermi approximation can be used in both the axial and the transverse directions, while in many cases of practical interest this approximation is only valid for the axial dynamics.

As is usual, we consider potentials of the form of the equation (3). If we substitute this potential and Eqs. (26) and (28) into (25), we find

$$
\begin{aligned}
i\hbar\frac{\partial}{\partial t}\left[\varphi(\vec{r}_\perp;n_1)\Phi(z,t)\right] &= \left(-\frac{\hbar^2}{2m}\Delta + V(\vec{r}) + U_0 n_1\left|\varphi(\vec{r}_\perp;n_1)\right|^2\right)\varphi(\vec{r}_\perp;n_1)\Phi(z,t) \rightarrow \\
\rightarrow i\hbar\frac{\partial}{\partial t}\left[\Phi(z,t)\right]\varphi(\vec{r}_\perp;n_1) &= -\frac{\hbar^2}{2m}\varphi(\vec{r}_\perp;n_1)\frac{\partial^2}{\partial z^2}\Phi(z,t) - \frac{\hbar^2}{2m}\Phi(z,t)\Delta_\perp\varphi(\vec{r}_\perp;n_1) + \\
&+ (V_\perp(\vec{r}_\perp) + V_z(z))\varphi(\vec{r}_\perp;n_1)\Phi(z,t) + U_0 n_1\left|\varphi(\vec{r}_\perp;n_1)\right|^2\varphi(\vec{r}_\perp;n_1)\Phi(z,t) \rightarrow \\
&\rightarrow \left(i\hbar\frac{\partial}{\partial t}\Phi(z,t) + \frac{\hbar^2}{2m}\frac{\partial^2}{\partial z^2}\Phi(z,t) - V_z(z)\Phi(z,t)\right)\varphi(\vec{r}_\perp;n_1) = \\
&= \left(-\frac{\hbar^2}{2m}\Delta_\perp\varphi(\vec{r}_\perp;n_1) + V_\perp(\vec{r}_\perp)\varphi(\vec{r}_\perp;n_1) + U_0 n_1\left|\varphi(\vec{r}_\perp;n_1)\right|^2\varphi(\vec{r}_\perp;n_1)\right)\Phi(z,t),
\end{aligned}
\tag{29}
$$

where $\Delta_\perp = \frac{\partial^2}{\partial x^2} + \frac{\partial^2}{\partial y^2}$.
Then, if we multiply equation (29) by $\varphi^*(\vec{r}_\perp;n_1)$ and integrate on the transverse coordinates, taking into account that $\int d\vec{r}_\perp \left|\varphi(\vec{r}_\perp;n_1)\right|^2 = 1$, we obtain

$$
i\hbar\frac{\partial\Phi(z,t)}{\partial t} = \left(-\frac{\hbar^2}{2m}\frac{\partial^2}{\partial z^2} + V_z(z) + \mu_\perp\right)\Phi(z,t), \tag{30}
$$

which is the equation that governs the axial dynamics of the condensate. Here, we have defined

$$
\mu_\perp = -\frac{\hbar^2}{2m}\int d\vec{r}_\perp\left(\varphi^*(\vec{r}_\perp;n_1)\Delta_\perp\varphi(\vec{r}_\perp;n_1) + V_\perp(\vec{r}_\perp)\left|\varphi(\vec{r}_\perp;n_1)\right|^2 + U_0 n_1\left|\varphi(\vec{r}_\perp;n_1)\right|^4\right) \tag{31}
$$

Substituting Eq. (30) into Eq. (29), multiplying by $\Phi^*(z,t)$ and integrating on the axial coordinates, we obtain the equation that governs the transverse dynamics of the condensate

$$
\left(-\frac{\hbar^2}{2m}\Delta_\perp + V_\perp(\vec{r}_\perp) + U_0 n_1\left|\varphi(\vec{r}_\perp;n_1)\right|^2\right)\varphi(\vec{r}_\perp;n_1) = \mu_\perp\varphi(\vec{r}_\perp;n_1), \tag{32}
$$

4.2 Local Chemical Potential

The local chemical potential $\mu_\perp$ corresponds to the chemical potential associated to the transverse dynamics, which is justified by Eq. (32). Furthermore, if we apply

the Thomas-Fermi approximation in the axial coordinates, we find that $\mu = V_z + \mu_\perp$ [5, 6], so it can be interpreted as the transversal part of the total chemical potential μ.

To obtain the final form of Eq. (30), we only need to determine $\mu_\perp$. For condensates with $a_S > 0$ (repulsive interatomic interactions) $\mu_\perp$ is bounded from below, so we can use a variational approach in order to minimize the chemical potential functional given by the equation (31) to find an estimation for $\mu_\perp$ in the ground state [5, 6]. An approximation for $\varphi(\vec{r}_\perp; n_1)$ is needed to perform this variational treatment. Since we have for this kind of condensates $\mu \gtrsim \hbar\omega_\perp \gg \hbar\omega_z$, the quantum of energy in the transversal coordinates is of the order of the total energy of the system while the quantum of energy in the axial coordinates is much smaller. In consequence, there can be only a few possible excited states in the transverse direction, so the corresponding wave function is near the ground state of a harmonic oscillator characterized by $a_\perp$. Thus, we use the Gaussian function of the ground state, with a variational parameter α (which characterizes the width of the function), as an anzat:

$$\varphi(\vec{r}_\perp; n_1) = \frac{1}{\sqrt{\pi(\alpha a_\perp)^2}} e^{-\frac{r_\perp^2}{2(\alpha a_\perp)^2}} \tag{33}$$

Using this, we can minimize $\mu_\perp[\alpha]$ in terms of the variational parameter α. Before that, we need the following results [2]

$$\Delta_\perp \varphi(\vec{r}_\perp; n_1) = \left(\frac{\partial^2}{\partial r_\perp^2} + \frac{1}{r_\perp}\frac{\partial}{\partial r_\perp} + \frac{1}{r_\perp^2}\frac{\partial^2}{\partial \theta^2} \right) \varphi(\vec{r}_\perp; n_1) =$$

$$= \frac{1}{(\alpha a_\perp)^2} \left(\frac{r_\perp^2}{(\alpha a_\perp)^2} - 2 \right) \varphi(\vec{r}_\perp; n_1) \tag{34}$$

$$\int_{-\infty}^{\infty} d\vec{r}_\perp r_\perp^2 \varphi^2 = \int_0^\infty dr_\perp r_\perp^3 \varphi^2 = (\alpha a_\perp)^2 \tag{35}$$

$$\int_{-\infty}^{\infty} d\vec{r}_\perp \varphi^4 = \int_0^\infty dr_\perp r_\perp \varphi^4 = \frac{1}{2\pi(\alpha a_\perp)^2} \tag{36}$$

[2] Here, we have used

$$\int_0^\infty x^m e^{-ax^2} dx = \frac{\Gamma\left[\frac{m+1}{2}\right]}{2a^{(m+1)/2}}$$

$$\Gamma(n+1) = n!, \text{ if } n \text{ is integer.}$$

Substituting Eqs. (34)–(36) into Eq. (31), and using that $\int d\vec{r}_\perp \left|\varphi\right|^2 = 1$, we obtain

$$\mu_\perp = \left(\frac{\hbar^2}{2m} + \frac{U_0 n_1}{2\pi}\right)(\alpha a_\perp)^{-2} + \frac{1}{2}m\omega_\perp^2(\alpha a_\perp)^2, \tag{37}$$

and differentiating with respect to α and setting to zero

$$\alpha = \sqrt[4]{1 + 4a_S n_1}, \tag{38}$$

where we have used the definition of U_0 and the oscillator length $a_\perp$.
With this result, we find the following estimation for $\mu_\perp$:

$$\mu_\perp = \hbar\omega_\perp\sqrt{1 + 4a_S n_1} \equiv \hbar\omega_\perp\sqrt{1 + 4a_S N\left|\Phi(z,t)\right|^2}, \tag{39}$$

so the final quasi-onedimensional equation governing the axial dynamics of the condensate becomes:

$$i\hbar\frac{\partial\Phi(z,t)}{\partial t} = \left[-\frac{\hbar^2}{2m}\frac{\partial^2}{\partial z^2} + V_z(z) + \hbar\omega_\perp\sqrt{1 + 4a_S N\left|\Phi(z,t)\right|^2}\right]\Phi(z,t) \tag{40}$$

5 Numerical Calculation

Una vez obtenidos los resultados para el caso quasi-unidimensional, procedemos a la parte numérica del trabajo. En este apartado, se llevan a cabo las adimensionalizaciones necesarias para poder trabajar con las ecuaciones numéricamente. Tras esto, se utilizan y explican el método de Crank-Nicolson y el algoritmo de Thomas, necesarios para la construcción posterior del código en Python. Finalmente, se presentan las ecuaciones con las que se compararán los resultados calculados por el programa.

5.1 Dimensionless Equations

Before carrying out the numerical treatment, we need to get the dimensionless equations we are going to use. Working with dimensionless quantities will allows us to identify the physical variables relevant to the problem as well as their typical range of values. In particular, it will allows us to estimate the proper space and time numerical steps.
In this work we will express lengths in units of a_z, energies in units of $\hbar\omega_z$, and time in units of ω_z^{-1}, which leads to the following dimensionless quantities

$$\tilde{z} = \frac{z}{a_z} \rightarrow \frac{\partial}{\partial \tilde{z}} = a_z \frac{\partial}{\partial z} \rightarrow \frac{\partial^2}{\partial \tilde{z}^2} = a_z^2 \frac{\partial^2}{\partial z^2} \tag{41}$$

$$\tilde{t} = \omega_z t \rightarrow \frac{\partial}{\partial \tilde{t}} = \frac{1}{\omega_z} \frac{\partial}{\partial t} \tag{42}$$

$$\tilde{\Phi}(\tilde{z}, \tilde{t}) = \sqrt{a_z}\Phi(z, t) \tag{43}$$

$$\tilde{V}_z(\tilde{z}) = \frac{V_z(z)}{\hbar\omega_z} = \frac{\tilde{z}^2}{2} \tag{44}$$

Substituting Eqs. (41)–(44) in Eq. (40), dividing by $\hbar\omega_z$ and using the definition of a_z, we find the dimensionless quasi-onedimensional equation

$$i\frac{\partial \tilde{\Phi}(\tilde{z}, \tilde{t})}{\partial \tilde{t}} = \left[-\frac{1}{2}\frac{\partial^2}{\partial \tilde{z}^2} + \tilde{V}_z(\tilde{z}) + \frac{\omega_\perp}{\omega_z}\sqrt{1 + 4\frac{a_S}{a_z}N\left|\tilde{\Phi}(\tilde{z}, \tilde{t})\right|^2} \right] \tilde{\Phi}(\tilde{z}, \tilde{t}) \tag{45}$$

We also need the total chemical potential functional. Since the axial wave function depends explicitly on time, using stationary states of the form $\Psi(\vec{r}, t) = \phi(\vec{r})e^{-i\mu t/\hbar} \rightarrow$

$\Phi(z,t) = \Phi(z)e^{-i\mu t/\hbar}$, we obtain

$$\mu[\Phi,\Phi^*] = \int_{-\infty}^{\infty} dz\Phi^*(z)\left(-\frac{\hbar^2}{2m}\frac{\partial^2}{\partial z^2} + V_z(z) + \hbar\omega_\perp\sqrt{1+4a_S N\left|\Phi(z)\right|^2}\right)\Phi(z), \quad (46)$$

where we have substituted the stationary state into the equation (40), multiplied by $\Phi(z)^*$ and integrated on z.
Repeating the procedure to obtain Eq. (45), we find the dimensionless chemical potential

$$\tilde{\mu}[\tilde{\Phi},\tilde{\Phi}^*] = \int_{-\infty}^{\infty} d\tilde{z}\tilde{\Phi}^*(\tilde{z})\left(-\frac{1}{2}\frac{\partial^2}{\partial\tilde{z}^2} + \tilde{V}_z(\tilde{z}) + \frac{\omega_\perp}{\omega_z}\sqrt{1+4\frac{a_S}{a_z}N\left|\tilde{\Phi}(\tilde{z})\right|^2}\right)\tilde{\Phi}(\tilde{z}) \quad (47)$$

5.2 Crank-Nicolson Method and Thomas Algorithm

Now, we need to make approximations to transform equations (45) and (47) into equations that can be used for numerical calculation[3]. We use for this a Crank-Nicolson method, which approximate the derivatives by finite differences. In this context, we define a temporal and spatial grid, where our system is placed, defined by the temporal step $t_{n+1} - t_n$ and the spatial step $z_{j+1} - z_j$.
We write $\Phi(z_j, t_n)$ as Φ_j^n and develop $\Phi_{j\pm1}^n$ and Φ_j^{n+1} as Taylor series centered at z_j, t_n

$$\Phi_{j+1}^n = \Phi_j^n + \partial_j\Phi_j^n(z_{j+1} - z_j) + \frac{1}{2}\partial_j^2\Phi_j^n(z_{j+1} - z_j)^2 + ... \quad (48)$$

$$\Phi_{j-1}^n = \Phi_j^n - \partial_j\Phi_j^n(z_j - z_{j-1}) + \frac{1}{2}\partial_j^2\Phi_j^n(z_j - z_{j-1})^2 + ... \quad (49)$$

$$\Phi_j^{n+1} = \Phi_j^n + \partial_n\Phi_j^n(t_{n+1} - t_n) + ..., \quad (50)$$

where we have denoted

$$\partial_j f_j^n \equiv \frac{\partial f_{j\pm1}^n}{\partial z_{j\pm1}}|_{z_{j\pm1}=z_j} \equiv \frac{\partial f_j^n}{\partial z_j} \quad (51)$$

$$\partial_j^2 f_j^n \equiv \frac{\partial^2 f_{j\pm1}^n}{\partial z_{j\pm1}^2}|_{z_{j\pm1}=z_j} \equiv \frac{\partial^2 f_j^n}{\partial z_j^2} \quad (52)$$

$$\partial_n f_j^n \equiv \frac{\partial f_j^{n+1}}{\partial t_{n+1}}|_{t_{n+1}=t_n} \equiv \frac{\partial f_j^n}{\partial t_n} \quad (53)$$

[3]From here on, the *tildes* are going to be omitted because from this point, we are going to work only with the dimensionless equations.

Truncating Eqs. (48) and (49) to second order and summing them, we obtain the spatial derivative approximation

$$\frac{\partial^2 \Phi_j^n}{\partial z_j^2} = \frac{\Phi_{j+1}^n - 2\Phi_j^n + \Phi_{j-1}^n}{\Delta z^2} \tag{54}$$

where $\Delta z = (z_j - z_{j-1})$ is the spatial step. Similarly, truncating Eq. (50) to first order, we can obtain the time derivative approximation

$$\frac{\partial \Phi_j^n}{\partial t_n} = \frac{\Phi_j^{n+1} - \Phi_j^n}{\Delta t}, \tag{55}$$

with $\Delta t = (t_{n+1} - t_n)$ being the time step.
Using these results, Eq. (45) takes the form

$$\begin{aligned} \Phi_j^{n+1} &= \left(\delta_{kj} - i\Delta t H_{kj}^n\right) \Phi_k^n \rightarrow \\ \rightarrow \Phi^{n+1} &= \left(\mathbb{1} - i\Delta t H^n\right) \Phi^n, \end{aligned} \tag{56}$$

where we have defined:

$$H_{kj}^n = -\frac{1}{2\Delta z^2}\left(\delta_{kj+1} - 2\delta_{kj} + \delta_{kj-1}\right) + \frac{z_j^2}{2}\delta_{kj} + \frac{\omega_\perp}{\omega_z}\sqrt{1 + 4\frac{a_S}{a_z} N \left|\Phi_j^n\right|^2}\delta_{kj}, \tag{57}$$

$$\Phi^n = \begin{bmatrix} \Phi_1^n \\ \vdots \\ \Phi_M^n \end{bmatrix} \tag{58}$$

Now, comparing the equation (56) with the series of an exponential function $e^x = \sum_{n=0}^{\infty} \frac{x^n}{n!}$, we can write at first order

$$\Phi^{n+1} = e^{-i\Delta t H^n} \Phi^n = \left(e^{i\frac{\Delta t}{2} H^n}\right)^{-1} e^{-i\frac{\Delta t}{2} H^n} \Phi^n, \tag{59}$$

and going back to the series expansion at first order

$$\Phi^{n+1} = \left(\mathbb{1} + i\frac{\Delta t}{2} H^n\right)^{-1} \left(\mathbb{1} - i\frac{\Delta t}{2} H^n\right) \Phi^n = \left(\frac{1}{Q'^n} - \mathbb{1}\right) \Phi^n \equiv \Upsilon^n - \Phi^n, \tag{60}$$

where we have called $Q'^n = \frac{1}{2}\left(\mathbb{1} + i\frac{\Delta t}{2} H^n\right)$.
This equation can be obtained too as an average between an explicit Euler method and an implicit Euler method. Here, we have deduced it using approximations of

exponential functions at first order, which can be interpreted in terms of evolution operators acting on the wave function.
We will look for the stationary states of the condensates by using the imaginary time method which essentially consists in making the change $\Delta t \to -i\Delta t$ in the evolution operator. It can be easily seen that for a linear system governed by a Hamiltonian H, satisfying the eigenvalue equation $H\mathscr{S}_k = E_k\mathscr{S}_k$, the evolution in imaginary time leads to the ground state of the system. Indeed, starting from any normalized wave function $\Phi(0)$, one has

$$\Phi(t) = e^{-tH}\Phi(0) \equiv e^{-tH}\sum_k c_k\mathscr{S}_k = \sum c_k e^{-tE_k}\mathscr{S}_k \tag{61}$$

Thus, as t increases the higher modes decay more rapidly than the lower ones, so, eventually, only the lowest-energy stationary state survives.
Since the stationary states of a nonlinear Hamiltonian are not necessary orthonormal, justifying the validity of the imaginary time method for this kind of systems is more involved. However, as shown in Ref. [7], this method is also applicable to nonlinear systems. In this case, Eq. (60) becomes

$$\Phi^{n+1} = \left(\frac{1}{Q^n} - \mathbb{1}\right)\Phi^n \equiv \Upsilon^n - \Phi^n, \tag{62}$$

where $Q^n = \frac{1}{2}\left(\mathbb{1} + \frac{\Delta t}{2}H^n\right)$.
Solving the equation above requires to solve the equation $Q^n\Upsilon^n = \Phi^n$ for Υ^n, which is a simple task because Q is a tridiagonal matrix.
This simple kind of equation system can be solved by using the Thomas algorithm. Writing the matrices as

$$Q^n = \begin{bmatrix} a_1 & b_1 & 0 & ... & 0 \\ c_2 & a_2 & b_2 & ... & 0 \\ \vdots & \ddots & \ddots & \ddots & \vdots \\ 0 & ... & c_{M-1} & a_{M-1} & b_{M-1} \\ 0 & ... & 0 & c_M & a_M \end{bmatrix}, \qquad \Upsilon^n = \begin{bmatrix} \Upsilon_1^n \\ \vdots \\ \Upsilon_M^n \end{bmatrix}, \qquad \Phi^n = \begin{bmatrix} \Phi_1^n \\ \vdots \\ \Phi_M^n \end{bmatrix}, \tag{63}$$

the Thomas algorithm can be summarized as

$$b_i' = \begin{cases} \frac{b_i}{a_i}, & i = 1 \\ \\ \frac{b_i}{a_i - c_i b_{i-1}'}, & i = 2, 3, ..., M-1 \end{cases} \tag{64}$$

$$\Phi_i'^n = \begin{cases} \frac{\Phi_i^n}{a_i}, & i = 1 \\ \frac{\Phi_i^n - c_i \Phi_{i-1}'^n}{a_i - c_i b_{i-1}'}, & i = 2, 3, ..., M \end{cases} \tag{65}$$

$$\begin{cases} \Upsilon_M^n = \Phi_M'^n \\ \Upsilon_i^n = \Phi_i'^n - b_i' \Upsilon_{i+1}^n, \quad i = M-1, M-2, ..., 1 \end{cases} \tag{66}$$

The Crank-Nicolson method is very stable (specially for imaginary time) and converges whenever the condition $\Delta t < \beta \Delta z^2$ is satisfied, where usually $\beta = 1/2$ [8]. Anyway, the best time and space steps can be found by trial and error.
On the other hand, the imaginary time method does not conserve the norm [7], so it is necessary to normalize in each iteration the wave function obtained.
Using the Crank-Nicolson method with imaginary time, we obtain the ground state wave function Φ for various condensates, and from this wave function we calculate the chemical potential μ by approximating the integral of Eq. (46) with the trapezoidal rule.
In order to calculate Φ, an initial trial wave function is needed. One could start, for instance, from the Gaussian function of the ground state of a harmonic oscillator of width a_z or from the Thomas-Fermi approximation for the axial wave function of the condensate. The larger N, the further the former function from the final result and the nearer the latter. Nevertheless, both functions eventually give converged solutions, the only difference being the number of iterations needed. In our case, we have chosen to start the iterations from the dimensionless Gaussian

$$\Phi^0(z) = \pi^{-\frac{1}{4}} e^{\frac{1}{2}z^2} \tag{67}$$

5.3 Reference Equations and Data

In order to check the results of the computer program, we will make use of the following analytical (dimensionless) expressions derived in Refs. [5, 6] that reproduce the results of the three-dimensional Gross-Pitaevskii equation with an accuracy typically better than 1% at least for $N \geqslant 1000$:

$$\mu = \frac{1}{\lambda} + \frac{L^2}{2} \tag{68}$$

$$a_S n_1(z) = \begin{cases} \frac{\lambda L^2}{4}\left(1-\frac{z^2}{L^2}\right) + \frac{\left(\sqrt{\lambda}L^2\right)^4}{16}\left(1-\frac{z^2}{L^2}\right)^2, & |z| < L \\ 0, & |z| > L \end{cases} \tag{69}$$

$$L = \frac{1}{\sqrt{\lambda}}\left(\frac{1}{(15\chi)^{4/5}+\frac{1}{3}} + \frac{1}{57\chi+345} + \frac{1}{(3\chi)^{4/3}}\right), \tag{70}$$

where L is the dimensionless axial half-length of the condensate, $\lambda = \omega_z/\omega_\perp$ and $\chi = \lambda N \frac{a_S}{a_\perp}$. It is worth noting that the parameter χ characterizes completely the ground state properties of the elongated condensate, so in order to test our program with different quasi-onedimensional BECs, it is sufficient to vary χ (for instance, by varying the number of particles N).

Since for elongated condensates $\omega_\perp \gg \omega_z$, we have $\lambda \ll 1$. In this work we take $\lambda = 0.1$, which corresponds to the most stringent case. Besides, in order to compare $|\Phi|^2$ with $a_S n_1$, we need to multiply by $\frac{a_S}{a_z}N$, since $a_S n_1 = \frac{a_S}{a_z} N |\Phi|^2$.

The calculations have been carried out for a ^{87}Rb condensate. In this case, we have

$$\begin{cases} a_i = \frac{10.784270}{\sqrt{\nu_i(Hz)}}(\mu m), \\ a_S = (5.29)10^{-3}(\mu m) \end{cases} \tag{71}$$

where ν_i ($i = \perp, z$), are the trap frequencies.

6 Python Program

En esta Sección se muestran y explican brevemente los programas desarrollados durante el trabajo. Primero, se presenta el programa principal, con el cual se obtienen el potencial químico y la función de onda del estado fundamental para distintos números de partículas. Luego, se desarrolla un programa capaz de resolver sistemas de ecuaciones de matrices tridiagonales siguiendo el algoritmo de Thomas. A pesar de que este programa en Python proporciona resultados correctos, hemos optado por usar la subrutina solve() en el programa principal, dado que resulta algo más rápida.

6.1 Program: Crank-Nicolson Method

When one runs this program, it asks for the following input data (as shown in Figs. 1 and 2):

- Number of particles.
- Transversal frequency in Hz ($\nu_\perp$).
- Starting iteration: The program is conceived in order to start from either the initial trial Gaussian function or from a (usually, not fully converged) wave function obtained in a previous run. In this latter case, one must specify the file where the wave function was saved. This option is useful because it permits us to refine previous results.
- Number of steps in L: Half of the number of spatial steps. Since L is determined by choosing N, it is sufficient to specify the desired number of steps to obtain Δz.
- Number of steps in time: It is the number of iterations of the method.
- Conversion factor: The program uses automatically the expression $\Delta t = f\frac{\Delta z^2}{2}$, where f is a factor that the user determines. It allows us to change the time step Δt.
- The names of the files where our results are saved (numerical μ and Φ). The program will create another file named '*Datos_entrada_*<fi file name>*.txt*', where all the input data are saved.

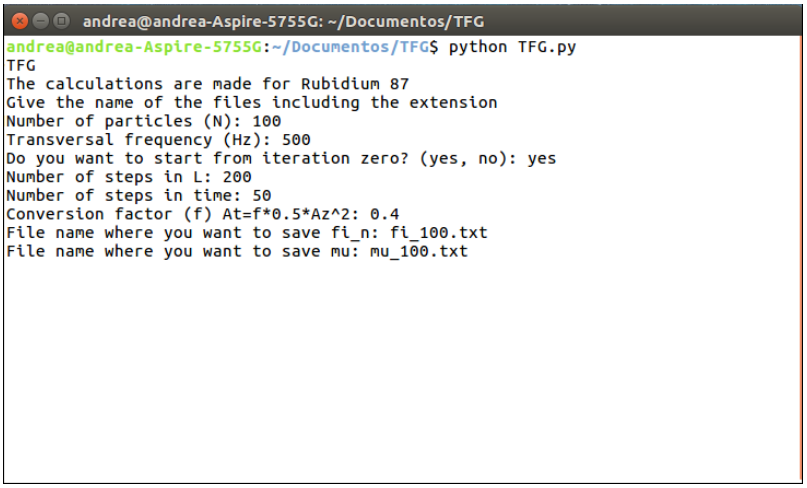

Figure 1: Terminal. Collecting data when starting from the first iteration.

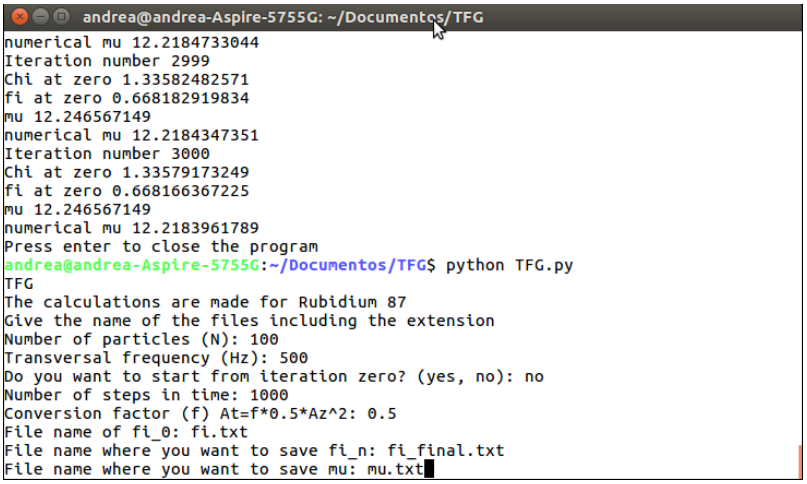

Figure 2: Terminal. Collecting data when starting from the wave function obtained in a previous iteration. We can also see above the end of the program.

With this input data, the program calculates the numerical approximation for Φ and μ and compares them to the theoretical predictions from the analytical expressions given in Section 5.3. The results for each iteration are displayed in the terminal (see Fig. 2) in order to check if the chosen parameters are adequate. If it is not the case, we can stop the program ($Ctrl+C$) and use another ones (the old ones are

specified in the file '*Datos_entrada_*<fi file name>*.txt*', so we can check it in order to make sure that we do not repeat any bad parameter).
Now, we show the code of the program:

```
#!/usr/bin/env python
# -*- coding: utf-8 -*-
#Pylab and scipy.linalg modules are imported
from pylab import *
import scipy.linalg as sl
#Data
print 'TFG\n' 'The calculations are made for Rubidium 87\n' 'Give the name of the files
including the extension'
a_1=raw_input('Number of particles (N): ')
a_2=raw_input('Transversal frequency (Hz): ')
a_6=raw_input('Do you want to start from iteration zero? (yes, no): ')
if a_6 == 'yes' or a_6 == 'Yes' or a_6 == 'YES':
    a_3=raw_input('Number of steps in L: ')
a_4=raw_input('Number of steps in time: ')
a_5=raw_input('Conversion factor (f) At=f*0.5*Az^2: ')
if a_6 == 'no' or a_6 == 'No' or a_6 == 'NO':
    a_7=raw_input('File name of fi_0: ')
    f=loadtxt('/home/andrea/Documentos/TFG/% s'%a_7, skiprows=1)#If we are not start-
ing in iteration zero, this is the file were fi_0 is.
    fi_0=f[:,1]
    z=f[:, 0]
    a_3=size(z)/2. -1
    Az=z[1]-z[0]
a_8=raw_input('File name where you want to save fi_n: ')#z, fi
a_9=raw_input('File name where you want to save mu: ')#Iteration number, mu
if a_6 == 'no' or a_6 == 'No' or a_6 == 'NO':
    datos=loadtxt('/home/andrea/Documentos/TFG/%s'%a_9, skiprows=1)
    it=datos[:, 0]
    a_12=it[-1] +1
if a_6 == 'yes' or a_6 == 'Yes' or a_6 == 'YES':
    #Create the new file if it is iteration zero
    fichero=open('%s'%a_9, 'w+')
    fichero.close
    a_3=int(a_3)
a_1=int(a_1)
a_2=float(a_2)
a_4=int(a_4)
a_5=float(a_5)
#Rubidio 87 data
N=a_1 #Number of particles
landa=0.1
wt=2*pi*a_2 #(Hz)
wz=wt*landa #(Hz)
at=10.784270/((wt/(2.*pi))**0.5) #micrometers
az=10.784270/((wz/(2.*pi))**0.5) #micrometers
aS=5.29*10**(-3) #micrometers
#Chi and L:
X=landa*N*(aS/at) #Chi
L=(landa**(-0.5))*( (1./((15*X)**(4./5) + (1./3))) + (1./(57*X + 345)) + (1./((3*X)**(4./3))))**(-
0.25) #Dimensionless axial half-length
#Spatial and temporal steps
```

```
if a_6 == 'yes' or a_6 == 'Yes' or a_6 == 'YES':
    Az=(L+2)/a_3#Spacial
    z=arange(-2-L, L+2+Az, Az) #Frame centered in the center of the condensate
At=a_5*0.5*Az**2#Temporal
T=a_4
t=arange(0, T)
#Analytical mu and n_1
mu=(1./landa+0.5*(L)**2) # chemical potential (dimensionless, wz )
Z=arange(-L, L+Az, Az)
n=((landa*(L)**2)/(4))*(1.-((Z**2)/(L**2))) + (((L*landa**(0.5))**4)/(16))*(1.-((Z**2)/(L**2)))**2
#Actually, it is aS*n1, but it is simpler this way
n[0]=0
n[-1]=0
#Fi_0 Gaussian anzat:
if a_6 == 'yes' or a_6 == 'Yes' or a_6 == 'YES':
    fi_0=((pi)**(-0.25))*e**(-0.5*z**2)
    a_12=0
fi_0[0]=0
fi_0[-1]=0#Boundery conditions
#Create a file with the data
fichero=open('Datos_entrada_ %s'%a_8, 'a')
fichero.write('N=%i\n'%N)
fichero.write('v_t=%f\n'%a_2)
fichero.write('M=%i\n'%a_3)
fichero.write('n=%i\n'%a_4)
fichero.write('convert. fact. (f) At=f*0.5*Az^2: %f\n'%a_5)
fichero.write('At=%f\n'%At)
fichero.write('Az=%f\n'%Az)
fichero.close
#Cronecker's delta:
def delta(u,v):
    if u==v:
        return 1
    elif u!=v:
        return 0
#Function that returns the diagonals:
def diago(A):
    O=shape(A)
    d=array([])
    for i in arange(0, O[0]):
        d=concatenate((d, array([A[i, i]])))
    return d
def diag_sup(A):
    O=shape(A)
    d=array([])
    for i in arange(0, O[0]-1):
        d=concatenate((d, array([A[i, i+1]])))
    return d
def diag_inf(A):
    O=shape(A)
    d=array([])
    for i in arange(1, O[0]):
        d=concatenate((d, array([A[i, i-1]])))
    return d
#Iterations:
ion()
fi=fi_0
```

```
iteracion=0
for l in arange(0, size(t)):
    print 'Iteration number %i' % iteracion
    iteracion=iteracion+1
    Q=array([])
    for i in arange(0, size(z)):
        for j in arange(0, size(z)):
            H=-(0.5/(Az**2))*(delta(i,j-1)-2*delta(i,j) + delta(i,j+1)) + (0.5*(z[j])**2 +
(1./landa)*(1 + 4*(aS/az)*N*(fi[j]*fi[j]))**(0.5))*delta(i,j)
            Q=concatenate((Q, array([0.5*(delta(i,j)+(At*0.5)*H)])))
    Q=reshape(Q, (size(z), size(z)))
    q_1=concatenate((array([0]), diag_sup(Q)))
    q_2=diago(Q)
    q_3=concatenate((diag_inf(Q), array([0])))
    brian=array([q_1, q_2, q_3])
    freddy=sl.solve_banded((1, 1), brian, fi)#Q**(-1) * fi
    print 'Chi at zero', freddy[size(z)/2]
    fi=freddy-fi
    fi[0]=0
    fi[-1]=0#Boundery conditions
    #Calculation of the norm:
    Norma=0
    for v in arange(0, size(fi)):
        Norma=Norma+Az*fi[v]*fi[v]
    fi=fi/(Norma)**(0.5)
    print 'fi at zero', fi[size(z)/2]
    muu=0
    for k in arange(0, size(z)-1):
        y=(-(0.5/(Az**2))*(fi[k+1]-fi[k])**2)+(0.5*(z[k])**2+(1./landa)*(1+4*N*(aS/az)*fi[k]*fi[k])**0.5)*fi[k]*fi[k]
        muu=muu+y*Az
    print 'mu', mu
    print 'numerical mu', muu
    #Mu file
    fichero=open('%s'%a_9, 'a')
    fichero.write('%s %f\n'%(l+a_12,muu))
    fichero.close
#Last fi file
fichero=open('%s'%a_8, 'w+')
fichero.close
for i in arange(0, size(fi)):
    fichero=open('%s'%a_8, 'a')#
    fichero.write('%f %f\n'%(z[i], fi[i]))
    fichero.close
#Plot of the wave function (grosso modo)
fig, ax1 = subplots()
grid()
left, bottom, width, height = [0.7, 0.65, 0.25, 0.3]
ax2 = fig.add_axes([left, bottom, width, height])
#Big plot
#ax1.plot(array([Z[0], Z[1]]), array([n[0], n[1]]), 'r', label= r'$N \frac{a_S} {a_z} \left —
\phi ∧0 \right — ∧2$')
ax1.plot(Z, n, color='mediumseagreen', label=r'$a_s n_1$', linewidth=1.5)#aS*n1
jack=N*(aS/az)
ax1.plot(z, jack*fi*fi, '-.', color='k', label=r'$N \frac{a_S} {a_z} \left | \phi∧ { %i} \right |
∧2$'%(T+a_12+1), linewidth=2)#N*(aS/az)*(Modulo de fi)
xlabel('z', fontsize=16)
#Little plot
```

```
grid()
ax2.plot(Z, n, color='mediumseagreen', linewidth=1.5, label=r'$a_s n_1$')#aS*n1
jack=N*(aS/az)
ax2.plot(z, jack*fi*fi, '-.', color='k', linewidth=2, label=r'$N \frac{a_S} {a_z} \left | \phi ∧
{ %i} \right | ∧2$'%(T+a_12+1))#N*(aS/az)*(Modulo de fi)
fi_0=((pi)**(-0.25))*e**(-0.5*z**2)
ax2.plot(z, jack*fi_0*fi_0, color='red', linewidth=1.5, label= r'$N \frac{a_S} {a_z} \left |
\phi ∧0 \right | ∧2$')#N*(aS/az)*(Modulo de fi_0)
legend(loc='best')
#ploteo mu
datos=loadtxt('/home/andrea/Documentos/TFG/%s'%a_9, skiprows=1)
l=datos[:, 0]
muu=datos[:, 1]
figure(2)
grid()
axhline(mu, color='r', linewidth=1.5, label=r'$ \mu $')
plot(l, muu, '-k', label=r'$ \mu_ {numerical} $', linewidth=1.5)
text((T+a_12)/2., (muu[0]-mu)/2. +1 +mu, '%f'%muu[-1])
text((T+a_12)/2., (muu[0]-mu)/2. +mu, '%f'%mu, color='r')
legend(loc='best')
xlabel(r'$Iteration$ $number$', fontsize=16)
ylabel(r'$ \mu $', fontsize=16)
a=raw_input('Press enter to close the program')
```

6.2 Program: Thomas Algorithm

The subroutine *solve*() (from the Scipy.linalg library) used in the program above, uses the three diagonals of the matrix Q^n and the matrix Υ^n as input data in order to solve the tridiagonal system of equations. For this purpose, we have also created an analogue function that takes the same input data based on the Thomas algorithm:

```
#Now, we need to write q_i as:
q_1=concatenate((array([0]), diag_sup(Q)))
q_2=diago(Q)
q_3=concatenate((diag_inf(Q), array([0])))
#Here is the Thomas algorithm:
def thomas(q_1, q_2, c q_3, fi):
    A=size(fi)
    q_1[0]=q_1[0]/q_2[0]
    for i in arange(1, A-1):
        q_1[i]=q_1[i]/(q_2[i]-q_1[i-1]*q_3[i])
    fi[0]=fi[0]/q_2[0]
    for j in arange(1, A):
        fi[j]=(fi[j]-q_3[j]*fi[j-1])/(q_2[j]-q_1[j-1]*q_3[j])
    x=concatenate((ones(A-1), array([fi[-1]])))
    U=arange(0, A-1)
    UU=U[::-1]
    for k in UU:
        x[k]=fi[k] - q_1[k]*x[k+1]
    return x
```

7 Results and Discussion

Se muestran en este apartado los resultados obtenidos por el programa para diferentes números de partículas N, dentro del rango de validez de las ecuaciones presentadas en la Sección 5.3. En concreto, se calculan el potencial químico μ y la función de onda Φ para N=1000, N=10000, N=100000 y N=1000000, y se comparan con los resultados analíticos del potencial químico μ y la densidad local por unidad de longitud n_1 respectivamente.

In this Section, we show the numerical results obtained from our computer program for condensates with different number of particles N within the range of validity of the equations of motion derived in previous Sections ($N \gg 1$). In particular, we calculate the chemical potential μ and the wavefunction Φ for the ground state of elongated condensates with N=1000, N=10000, N=100000 and N=1000000. The

numerical results for the chemical potential compared with the corresponding theoretical predictions obtained from the analytical expression (68), are displayed in Fig. 3. As shown in the figure, numerical and theoretical results agree, for the different values of N, within 0.236%, 0.089%, 0.094% and 0.033%, respectively.

The calculations were made for condensates in a trap with radial frequency $\nu_\perp =$ 500Hz and aspect ratio $\lambda = \omega_z/\omega_\perp = 0.1$ and for 1000 iterations, which is more than enough, because all the results are fully converged before 600 iterations, as we can see in the plots.
In each case, we choose the proper spatial step: In ascending order of N, $\Delta z = \frac{L}{80}$, $\Delta z = \frac{L}{80}$, $\Delta z = \frac{L}{150}$ and $\Delta z = \frac{L}{150}$. We do the same for the temporal step: For N=1000 and N=10000 we choose $\Delta t = \frac{\Delta z^2}{2}$, for N=100000, $\Delta t = 0.5\frac{\Delta z^2}{2}$ and for N=1000000, $\Delta t = 0.1\frac{\Delta z^2}{2}$.

The numerical results for the square of the norm of Φ^n multiplied by $\frac{a_S}{a_z}N$ compared with the dimensionless analytical local density per unit length $a_S n_1$ (see Eq. (69)) are displayed in Figs. 4 and 5. As is apparent, the agreement is excellent.

Figure 6 shows a comparison between the numerical chemical potential μ and the corresponding analytical prediction as a function of the number of particles N. Similarly, Fig. 7 compares numerical and analytical results for the condensate peak density as a function of N. As can be seen from the figures, the agreement is again excellent, which proves the validity of our computer codes.

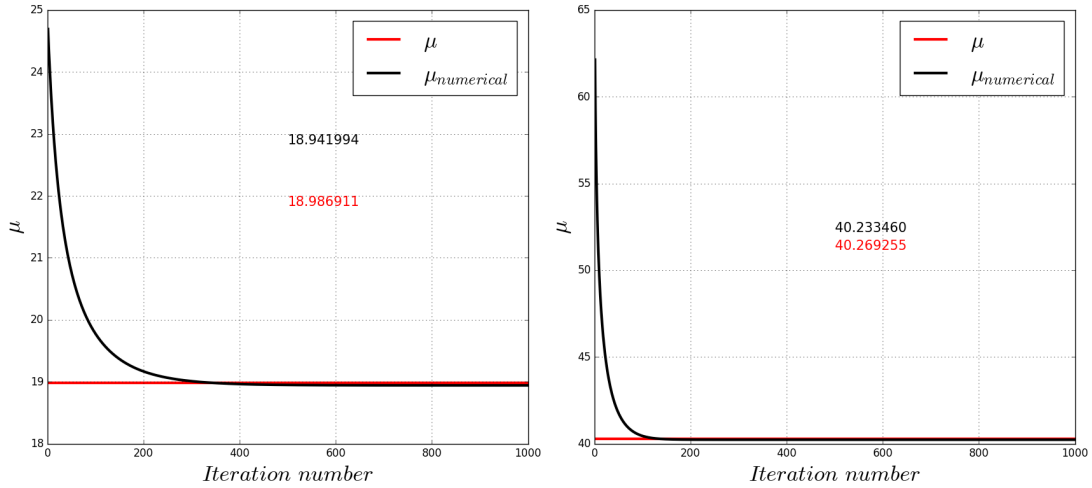

(a) N=1000 (b) N=10000

(c) N=100000 (d) N=1000000

Figure 3: Numerical calculations for μ (black) are compared with the corresponding analytical predictions (red) for the different values of N. The final value of the converged solution of the numerical chemical potential and that obtained from the analytical expression (68) are also shown.

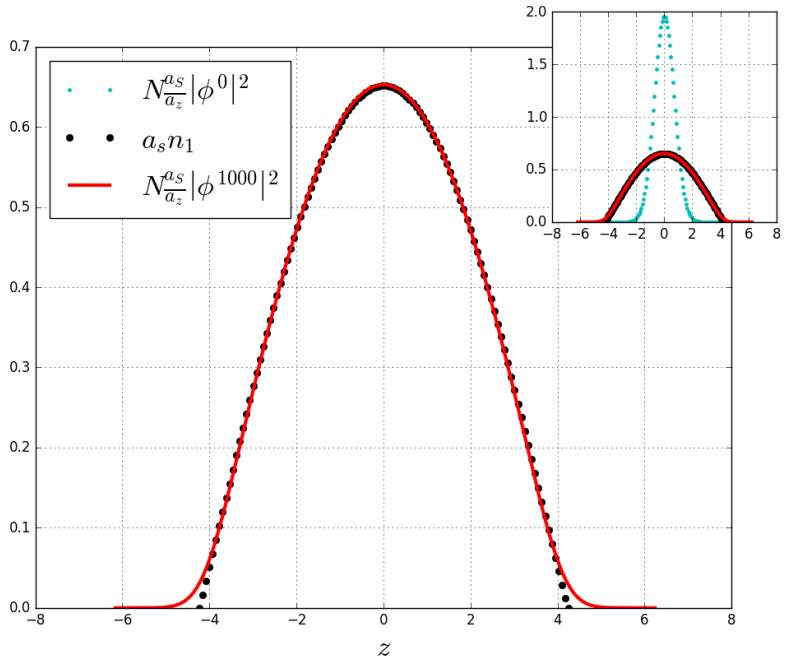

(a) N=1000

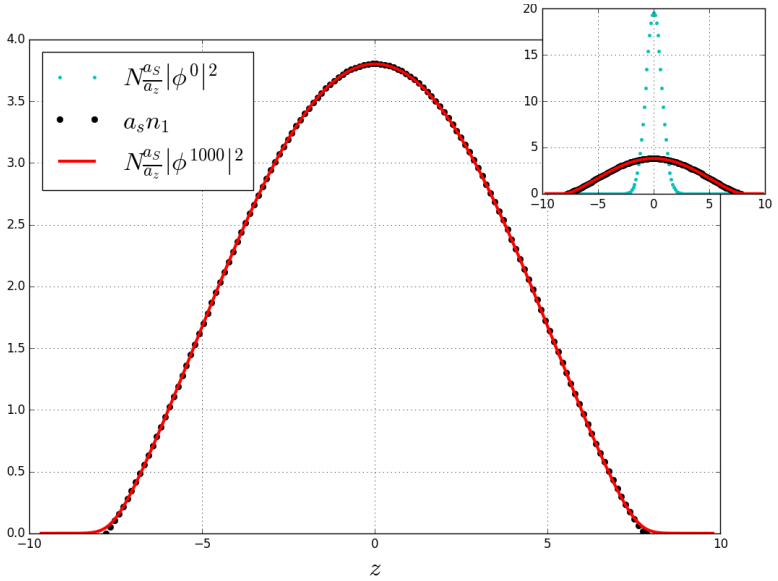

(b) N=10000

Figure 4: Module of the wave funtions (I). Numerical calculation for $\frac{a_S}{a_z} N \left|\Phi^n\right|^2$ (red), for $N = 1000$ (a) and $N = 10000$ (b), in comparison with the analytical calculation of $a_S n_1$ (black). In the right corner it is shown the squared norm of the Gaussian function used for starting the iterations multiplied by the same factor, $\frac{a_S}{a_z} N \left|\Phi^0\right|^2$ (blue).

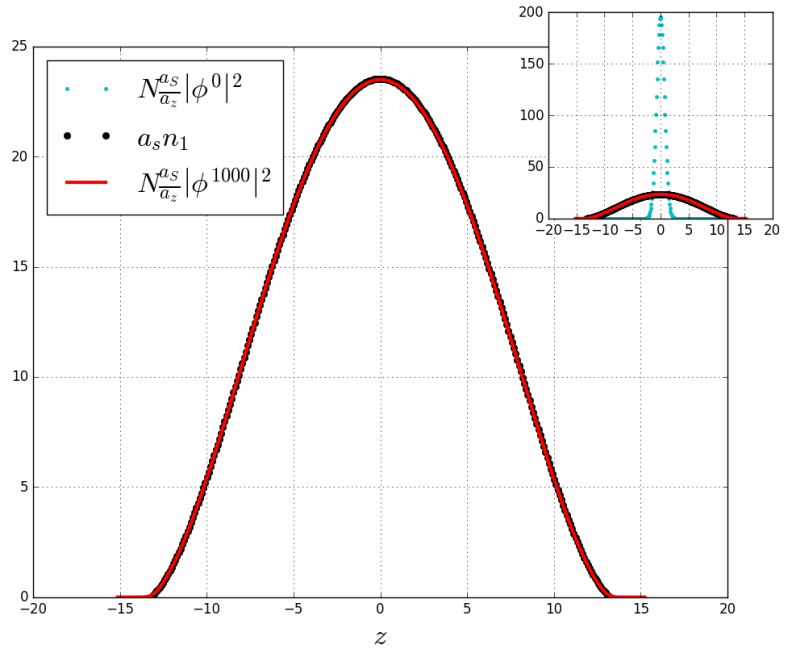

(a) N=100000

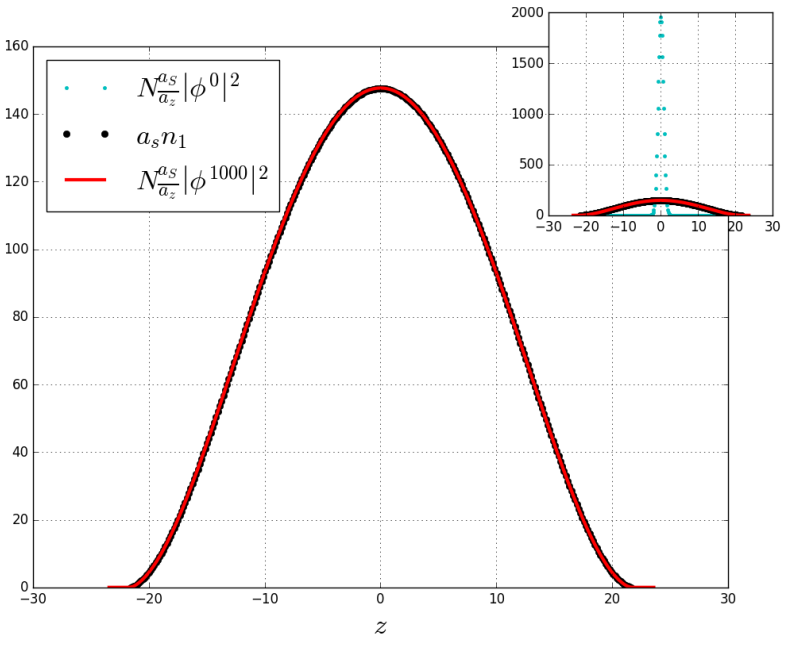

(b) N=1000000

Figure 5: Module of the wave funtions (II). Same as Fig. 4, for $N = 100000$ (a) and $N = 1000000$ (b).

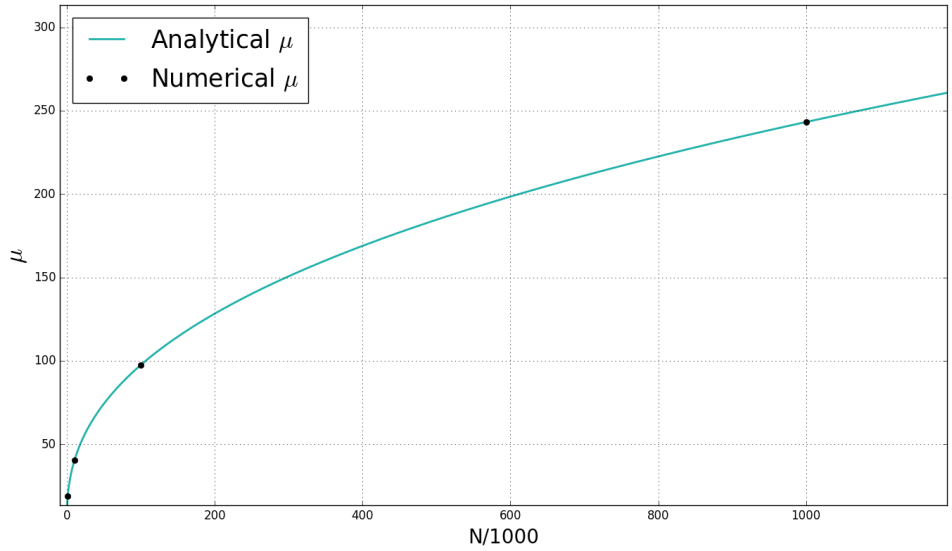

Figure 6: Comparison between the numerical chemical potential μ (black dots) and the corresponding analytical prediction (blue curve) as a function of the number of particles N.

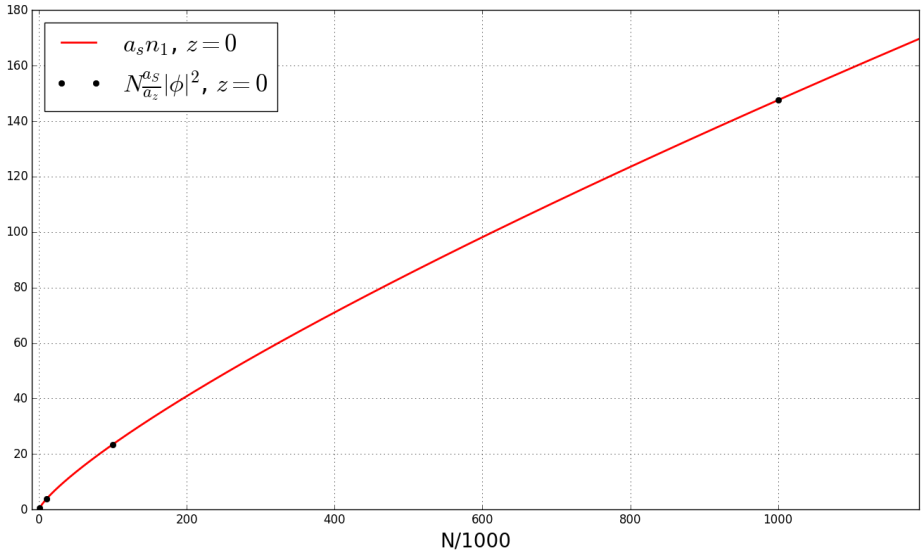

Figure 7: Comparison between the numerical peak density (black dots) and the corresponding analytical prediction $a_S n_1$ (red curve) as a function of the number of particles N.

8 Conclusions

En este trabajo, hemos dado una introducción teórica a la condensación de Bose-Einstein, desarrollando las ideas claves en torno a este fenómeno, describiendo las condiciones necesarias para producirlos y explicando los métodos utilizados para obtenerlos y sus aplicaciones. Hemos derivado la ecuación de Gross-Pitaevskii, que nos da una comprensión completa de la dinámica de cualquier condensado a temperatura $T = 0K$*. A partir de ella, hemos utilizado la aproximación adiabática para obtener las ecuaciones que gobiernan la dinámica de un condensado alargado.*
Finalmente, nos hemos centrado en este último caso y hemos aplicado técnicas numéricas para luego poder hacer un tratamiento computacional del problema, comparando los resultados obtenidos con soluciones analíticas. Hemos creado un programa capaz de calcular la función de onda del estado fundamental y el potencial químico de un condensado quasi-unidimensional, una vez aportados los datos del paso temporal y espacial. Este código también calcula las soluciones con las expresiones analíticas para comparar con nuestros resultados. En lo que a estos respecta, tal como hemos visto con anterioridad, nuestros programas consiguen precisiones mejores del 0.5%*, lo que demuestra su validez.*

In this work, we have provided a theoretical introduction to Bose-Einstein condensation. We have developed the main ideas about this phenomenon, describing the conditions needed in order to obtain them, the methods used to achieve these conditions, as well as their physical applications. We have derived the Gross-Pitaevskii equation, which fully describes the dynamics of any BEC at $T = 0K$. Based on this equation, we have used the adiabatic approximation in order to obtain the equations governing the dynamics of an elongated condensate.
Finally, we have focused on this latter case and applied numerical techniques in order to make a computational treatment of the problem, comparing our numerical results with the corresponding analytical predictions. We have created a computer program which is able to calculate both the ground state wave function and the chemical potential of cigar-shaped condensates. This program also calculates the analytical expressions in order to check the validity of our numerical code. In this regard, as already seen in previous Sections, our program provides results with an accuracy typically better than 0.5%, which proves its validity.

References

[1] Cohen-Tannoudji, Claude. *Condensation de Bose-Einstein des gaz atomiques ultra froids; effets des interactions*. Cours de physique atomique et moléculaire. Anneé 1998-1999, Collège de France.

[2] Dalfovo, F., Giorgini, S. Theory of Bose-Einstein condensation in trapped gases. *Rev. Mod. Phys.*, **71**, 463-512 (1999).

[3] Pethick, C. J., Smith, H. *Bose–Einstein Condensation in Dilute Gases*. United Kingdom: Cambridge University Press, 2002.

[4] Pitaevskii, L., Stringari, S. *Bose-Einstein Condensation*. United States: Oxford University Press, 2003.

[5] Muñoz Mateo, A., Delgado, V. Effective mean-field equations for cigar shaped and disk-shaped Bose-Einstein condensates. *Phys. Rev. A.*, **77**, 13617-13626 (2008).

[6] Muñoz Mateo, A., Delgado, V. Effective one-dimensional dynamics of elongated Bose-Einstein condensates. *Ann. Phys.*, **324**, 709-724 (2009).

[7] Chiofalo, M. L., Succi, S., Tosi, M.P. Ground state of trapped interacting Bose-Einstein condensates by an explicit imaginary-time algorithm. *Phys. Rev. E*, **62**, 7438-7444 (2000).

[8] Press, W. H., Teukolski, S. A., Vetterling, W. T., Flannery, B. P. *Numerical Recipes: The Art of Scientific Computing*. (3^{th} ed.) New York: Cambridge University Press, 2007.

[9] Muñoz Mateo, A. *Defectos topológicos en condensados de Bose-Einstein de gases atómicos confinados en trampas magneto-ópticas*. Ph. D. Doctoral thesis,

Universidad de La Laguna, La Laguna, 2012.

[10] Leggett, A. J. Bose-Einstein condensation in the alkali gases: Some fundamental concepts. *Rev. Mod. Phys.*, **73**, 307-356 (2001).

[11] Ketterle, W. Nobel lecture: When atoms behave as waves: Bose-Einstein condensation and the atom laser. *Rev. Mod. Phys.* **74**, 1131-1151 (2002).

[12] Inouye, S., Löw, R. F., Gupta, S., Pfau, T., Görlitz, A., Gustavson, T. L., Pritchard, D. E., Ketterle, W. Amplification of Light and Atoms in a Bose-Einstein Condensate. *Phys. Rev. Lett.*, **85**, 4225-4228 (2000).

[13] Burger, S., Bongs, K., Dettmer, S., Ertmer, W., Sengstock, K., Sanpera, A., Shlyapnikov, G. V., Lewenstein, M. Dark solitons in Bose-Einstein Condensates. *Phys. Rev. Lett.*, **83**, 5198-5201 (1999).